BBR NOV 2015

6 authors, including:

Murugappan M
Kuwait College of Science and Technology (A Private University), Kuwait

Norlinah Mohamed Ibrahim
UKM Medical Center

Edgar Mesquita
University of Minho

Behavioural Brain Research 298 (2016) 248–260

Contents lists available at ScienceDirect

Behavioural Brain Research

journal homepage: www.elsevier.com/locate/bbr

Research report

Brain functional connectivity patterns for emotional state classification in Parkinson's disease patients without dementia

R. Yuvaraj [a], M. Murugappan [b,*], U. Rajendra Acharya [c], Hojjat Adeli [d], Norlinah Mohamed Ibrahim [e], Edgar Mesquita [f]

[a] Department of Biomedical Engineering, Sri Sivasubramaniya Nadar (SSN) College of Engineering, Old Mahabalipuram Road, Kalavakkam, Chennai, 603110 Tamilnadu, India
[b] School of Mechatronic Engineering, University Malaysia Perlis (UniMAP), Campus Ulupauh, Arau, 02600 Perlis, Malaysia
[c] Department of Electronics and Computer Engineering, Ngee Ann Polytechnic, Singapore
[d] Departments of Biomedical Engineering, Biomedical Informatics, Civil, Environmental and Geodetic Engineering, Electrical and Computer Engineering, Neurology and Neuroscience Ohio State University, Columbus, OH 43210, USA
[e] Neurology Unit, Department of Medicine, UKM Medical Center, Jalan Yaacob Latiff, 56000 Bandar Tun Razak, Kuala Lumpur, Malaysia
[f] Department of Education, University of Minho, Braga, Portugal

HIGHLIGHTS

- Recognize different emotional states using brain functional connectivity.
- EEG change is significantly different among emotional states of PD patients.
- Highest classification results for the proposed bispectral functional connectivity index.
- PD patients exists decline in cortical connectivity during emotion processing.

ARTICLE INFO

Article history:
Received 16 August 2015
Received in revised form 16 October 2015
Accepted 20 October 2015
Available online 26 October 2015

Keywords:
EEG
Correlation
Coherence
PSI
Emotion
Parkinson's disease
SVM

ABSTRACT

Successful emotional communication is crucial for social interactions and social relationships. Parkinson's Disease (PD) patients have shown deficits in emotional recognition abilities although the research findings are inconclusive. This paper presents an investigation of six emotions (happiness, sadness, fear, anger, surprise, and disgust) of twenty non-demented (Mini-Mental State Examination score >24) PD patients and twenty Healthy Controls (HCs) using Electroencephalogram (EEG)-based Brain Functional Connectivity (BFC) patterns. The functional connectivity index feature in EEG signals is computed using three different methods: Correlation (COR), Coherence (COH), and Phase Synchronization Index (PSI). Further, a new functional connectivity index feature is proposed using bispectral analysis. The experimental results indicate that the BFC change is significantly different among emotional states of PD patients compared with HC. Also, the emotional connectivity pattern classified using Support Vector Machine (SVM) classifier yielded the highest accuracy for the new bispectral functional connectivity index. The PD patients showed emotional impairments as demonstrated by a poor classification performance. This finding suggests that decrease in the functional connectivity indices during emotional stimulation in PD, indicating functional disconnections between cortical areas.

1. Introduction

Parkinson's Disease (PD) is a progressive disorder which develops gradually and destroys the dopamine neurons in the substantia nigra pars compacta of the basal ganglia. The prime symptoms of the disease are tremor, muscular rigidity, bradykinesia, and postural instability. More studies are needed to understand the behavior by analyzing neural connectivities [1]. Studies have shown that subjects with PD have problems in deciphering emotions from speech [2,3] and facial expressions [4,5], display blunted startle eye-blink response to highly arousing unpleasant pictures [6,7] and blunted arousal ratings of highly arousing emotional pictures [8], although not all findings are consistent. A number of studies have not found any impaired performance on the recognition of facial emotions in their PD samples [9,10]. A few studies did not find any emotional deficits from prosody [11,12]. Altogether, research evidence from

* Corresponding author.
E-mail address: murugappan@unimap.edu.my (M. Murugappan).

http://dx.doi.org/10.1016/j.bbr.2015.10.036
0166-4328/© 2015 Published by Elsevier B.V.

the literature supports the covenant on emotional impairment in patients with PD. Most of the aforementioned studies have relied on information from behavioral measures of PD patients (e.g., recognition tasks) and very few with physiological measures (e.g., startle eye-blink reflex) for emotion recognition.

In the past few decades, numerous studies have been conducted to recognize emotion in healthy controls (HC) based on their facial expressions, speech, body gestures, and biosignals from autonomous nervous system (ANS), such as Heart Rate Variability (HRV), Electrodermal Response (EDR) and Galvanic Skin Response (GSR) [13–16]. Signals from central nervous system (CNS), namely electroencephalogram (EEG), Magnetoencephalogram (MEG) [17], Functional Magnetic Resonance Imaging (fMRI) and Positron Emission Tomography (PET) are more reliable for emotion recognition than other modalities [18]. For instance, the muscle tension in the face gives rise to facial actions, or for circumstances of social masking (example, an angry person may smile) [19]. PD patients may be unable to express their emotion via face. Similarly, speech signals convey emotional information depending on the manner in which it is delivered by the participant. The biosignals from ANS and/or CNS are usually not purposely controlled by the person and can deliver true inherent emotional state [20]. The ANS signals like GSR are highly influenced by inspiration from physical activity and not emotion. EEG is non-invasive and provides better time resolution than other CNS signals. However, most existing research on emotional EEG has focused on single-electrode EEG characteristic responses rather than an array of EEG electrodes in HC participant [21–23]. For example, Baumgartner et al. showed that EEG activity over the left hemisphere increases in happy conditions compared to negative emotional conditions [22].

Mauss and Robinson reported that emotional state involves circuits rather than isolated brain regions [24]. Several neuroimaging methods like fMRI, PET etc., are used to analyse interconnected neuronal activities in several brain regions to detect the emotions in the brain [25]. The authors advance the idea that brain functional connectivity (BFC) index using EEG is an appropriate method to analyse emotional specificity in PD patients compared to HC participant. Different techniques/indices have been used in the literature to measure brain functional connectivity [17,26–28]. The most commonly used methods for analysing emotional EEG between each pair of electrodes are: correlation (COR), coherence (COH) [29,30] and phase synchronization index (PSI) [31,32]. Shin and Park used correlation coefficients to analyse the changes in emotional status in HC participants according to the surrounding temperature [33]. They reported that the correlation coefficient is larger at high room temperatures in the temporal and the occipital regions while viewing negative emotional stimuli. Hinrichs and Machleidt showed a different degree of coherence in the alpha band, particularly, larger coherence in happiness than in sadness [34]. Miskovic and Schmidt report viewing of high emotionally arousing images increases the coherence between the prefrontal and posterior association cortices than neutral images [35]. Costa et al. reported an overall increase of synchronization index between right and left frontal sites while viewing sadness compared with happiness emotion [36]. These studies support the hypothesis that BFC using EEG can differentiate between different emotional states and these connectivity indices may provide a new insight for understanding the brain regions connectivity during emotional information processing in PD.

Recently, chaos theory and nonlinear methods have been used to obtain hidden information related to properties such as similarity, predictability, reliability and sensitivity of the physiological signals [37–40]. EEG is a non-linear, non-stationary and non-Gaussian signal. Emotions are transient event and the momentary variations in the EEG signals can be evaluated by understanding the non-linear behaviors present in signals. Higher order spectra (HOS) analysis is known to be an effective tool for the analysis of non-linear systems [41]. This paper proposes a bispectrum-based phase synchronization index (bPSI) as a tool to extract the functional connectivity alterations in PD patients compared to control subjects during emotion processing. The objectives of this study are, (a) to reveal whether emotional states can be categorized through BFC indices by predicting six emotions in PD patients; and (b) to compare the performance of COR, COH, and PSI with bPSI for recognition of emotional states of patients with PD.

A description of the materials, including participant's details, emotion elicitation stimuli and data acquisition procedure used in this study is presented in the next section. Then, the research methodology is presented followed by results. Finally, the limitations and conclusion of the study are summarized in the last two sections.

2. Materials used

2.1. Ethical approval

Prior to the study formal approval from University Kebangsaan Malaysia (UKM) medical center, ethics committee for human research (Ref. number: UKM1.5.3.5/244/FF-354-2012) was obtained. All participants/caretakers provided written informed consent prior to the experiment. Each participant was paid 50 Malaysian Ringgit (US $15) as participation honorarium.

2.2. Participants

Twenty non-demented patients with PD (10 females and 10 males; all right-handed) and twenty healthy control subjects (11 females and 9 males; all right-handed) are involved in this research. The subjects suffering from PD were selected from UKM medical hospital in Kuala Lumpur, Malaysia. All PD participants diagnosed by neurologists were under the influence of medication during the

Table 1
Background and neurophysiological characteristics (mean ± SD) of participants with PD and healthy controls.

Variables	PD	HC	Statistical test	*p*-value*
Sample size, *N*	20	20	NA	NA
Age, yr	59.05 ± 5.64	58.10 ± 2.95	$t = 0.667$	$p = 0.509$
Female/male	10/10	11/9	$x^2 = 0.100$	$p = 0.752$
Formal education, yr	10.45 ± 4.86	11.05 ± 3.34	$t = -0.455$	$p = 0.652$
Mini-mental state examination score (range: 0–30)	26.90 ± 1.51	27.15 ± 1.63	$t = -0.502$	$p = 0.619$
Beck depression Inventory scale (range: 0–21)	5.80 ± 2.87	5.45 ± 2.18	$t = -0.433$	$p = 0.667$
Edinburg handedness inventory (range: 1–10)	9.55 ± 0.76	9.84 ± 0.72	$t = -0.818$	$p = 0.403$
Hoehn & Yahr (stage: 1/2/3)	2.25 ± 0.63	NA	NA	NA
Unified Parkinson's disease rating scale	17.05 ± 3.15	NA	NA	NA
Duration of disease, yr	5.75 ± 3.52	NA	NA	NA

Note: *N*, number of participants; SD, standard deviation; NA, not applicable.
* Significant at $p < 0.05$.

Table 2
Significant results of F-test using correlation between the electrode pairs ($p < 0.05$) of PD patients and healthy controls.

Frequency band	PD patients						HC					
Alpha	AF3-P7	$F=2.15$	T7-FC6	$F=5.37$	T8-F4	$F=3.88$	F3-O2	$F=2.82$	T7-F8	$F=2.98$	T8-F8	$F=4.40$
	F3-P8	$F=1.09$	P7-T8	$F=3.31$	FC6-AF4	$F=2.20$	FC5-P8	$F=2.63$	P7-F4	$F=3.07$	F4–F8	$F=4.68$
			O2-F4	$F=2.68$	F8-AF4	$F=3.28$	FC5–FC6	$F=4.52$	O1–O2	$F=2.22$		
Beta	F7-O1	$F=2.36$	T7-P8	$F=6.03$	FC6-F8	$F=5.64$	AF3-FC6	$F=4.02$	P7–P8	$F=4.41$	F4-F8	$F=4.95$
	F3-P8	$F=4.09$	O1–O2	$F=2.36$	F4-F8	$F=3.46$	F7–F4	$F=3.65$	O1–O2	$F=2.27$	F8-AF4	$F=2.75$
	FC5-F4	$F=5.92$	O2-FC6	$F=5.09$			F3-O2	$F=3.35$	O2-P8	$F=4.43$		
							FC5-FC6	$F=4.68$				
Gamma	F3-O1	$F=2.70$	T7-FC6	$F=5.01$	T8-F4	$F=5.92$	F7-AF4	$F=4.76$	P7-T8	$F=6.52$	FC6-F4	$F=4.18$
	FC5-O2	$F=3.13$	P7-F4	$F=6.17$	FC6-F8	$F=6.88$	F3–F4	$F=5.49$	O1-FC6	$F=4.11$	F4-AF4	$F=2.46$
			O1-O2	$F=3.53$			FC6-FC6	$F=3.31$	O2-F4	$F=3.05$	F8-AF4	$F=4.20$

experiment. The average duration of the disease for PD subjects were about 5.75 years. Each PD patient was classified according to Unified Parkinson's Disease Rating Scale (UPDRS) and the Hoehn and Yahr (H & Y) severity measures. None of the patients had suffered by any other neurological or psychiatric disturbances that might independently influence their cognitive functioning besides PD.

The subjects from hospital's medical unit and/or from patient's relatives were engaged in this study as HC participant. The HC participant suffering from any psychiatric or neurological conditions were not included in this experiment. To exclude dementia or depression, participants scoring <24 on the Mini-Mental State Examination (MMSE) or >18 on the Beck Depression Inventory (BDI) were excluded [42]. Handedness was determined by self-report and confirmed by Edinburgh Handedness Inventory (EHI). Also, all participants were confirmed to have normal sight. Table 1 lists the summary of details of PD patients and control subjects. Patients and HC participants were homogeneous in terms of demographic variables such as age, gender distribution, and education level.

2.3. Stimuli used

The emotions of sadness, fear, and disgust were elicited using IAPS and IADS databases. The elicitation of happiness, surprise, and anger emotion was attained by using video clips (after a pilot study). A detailed description of the stimuli materials, experimental protocol, and procedure used in this experiment can be found in [43,44]. The emotional EEG signal is recorded with a 14-channel wireless (2.4 GHz band) Emotiv EPOC neuroheadset with a sampling frequency of 128 Hz. The electrodes are arranged at the scalp sites AF3, AF4, F7, F8, F3, F4, FC5, FC6, T7, T8, P7, P8, O1 and O2, according to the 10–20 system, referenced to linked ears.

3. Methodology

3.1. Signal pre-processing

The EEG signals with artifacts due to blinking are removed by discarding the amplitudes more than 80 μV [45]. Then butterworth sixth order bandpass filter is used to extract the five EEG frequency bands (delta (1–4 Hz), theta (4–8 Hz), alpha (8–13 Hz), beta (13–30 Hz), and gamma (30–49 Hz)) [43,46]. Each channel of EEG signals of emotions without artifacts is subdivided into segments of 6 s [43,44]. These EEG signals are used for analysis in this research.

3.2. Existing brain functional connectivity (BFC) indices

The brain functional connectivity using EEG between the recording sites is estimated following Costa et al. [36]. Five individual EEG frequency bands are analyzed for all pairwise combinations of 14 electrodes (total of 91 pairs).

3.2.1. Correlation

The correlation at specific frequency CPR(f), for two given signals S_1 and S_2 is defined as

$$\mathrm{COR}_{S_1S_2}(f) = C_{S_1S_2}(f)/\sqrt{C_{S_1S_1}C_{S_2S_2}} \tag{1}$$

where f denotes frequency, $C_{S_1S_2}$ indicates the cross-covariance of two given signals S_1 and S_2;$C_{S_1S_1}$ indicates the auto-covariance of given signal S_1; and $C_{S_2S_2}$ denotes the auto-covariance of given signal. Measure of correlation depends on both phase and polarity of the signal with a value varying between −1 and 1 [47]. A higher COR corresponds to stronger relationship between two different electrode sites of the scalp at a specific frequency.

Table 3
Significant results of F-test using coherence between the electrode pairs ($p < 0.05$) of PD patients and healthy controls.

Frequency band	PD Patients						HC					
Theta	F7-P8	$F=2.45$	T7–F8	$F=5.51$	P8-F4	$F=2.86$	F3-P8	$F=5.22$	T7–T8	$F=5.09$	P8-T8	$F=4.29$
	F3-O2	$F=2.99$	O2-FC6	$F=6.61$	T8-F8	$F=3.25$	FC5-T8	$F=2.85$	P7-02	$F=4.85$	T8-FC6	$F=3.64$
	FC5-P7	$F=3.54$							O1–02	$F=4.28$	F8-AF4	$F=5.46$
Alpha	AF3-AF4	$F=3.63$	T7-FC6	$F=3.22$	F4-AF4	$F=3.18$	AF3-AF4	$F=4.42$	T7–T8	$F=3.57$	FC6-F4	$F=4.99$
	F7–F8	$F=2.53$	P7-P8	$F=4.08$			F7–F4	$F=3.67$	T7-F8	$F=3.91$	F4–F8	$F=3.35$
	F3-O2	$F=4.53$	O1-O2	$F=2.76$			F3-P8	$F=2.65$	P7-F4	$F=4.41$		
	FC5-P8	$F=4.43$							O2-FC6	$F=5.56$		
Beta	F7–F8	$F=4.52$	P7-P8	$F=4.63$	P8-T8	$F=4.08$	F3–F4	$F=3.36$	P7-F4	$F=4.62$	P8-F8	$F=5.40$
	F3-O2	$F=4.45$	P7-F4	$F=4.64$	P8-FC6	$F=2.72$	F3-AF4	$F=3.50$	O1-T8	$F=3.38$	T8-F4	$F=3.44$
	F3-T8	$F=4.13$	O2-T8	$F=3.32$	FC6-F8	$F=3.22$	FC5-P8	$F=4.97$	O2-FC6	$F=3.25$	FC6-F8	$F=3.46$
											F8-AF4	$F=2.09$
Gamma	AF3-F8	$F=2.66$	T7-O2	$F=4.40$	FC6-F8	$F=5.40$	F7-F8	$F=2.79$	T7-T8	$F=3.13$	T8-F4	$F=3.64$
	F7-O1	$F=2.50$	T7-F8	$F=2.92$	F8-AF4	$F=4.31$	F3-T8	$F=5.30$	P7-FC6	$F=2.47$	F4–F8	$F=3.08$
	F7–F8	$F=1.17$	P7-T8	$F=3.14$			F3-AF4	$F=2.52$	O1-F4	$F=4.82$		
			O1-T8	$F=2.53$			FC5-P7	$F=3.78$	O2-F4	$F=5.86$		

3.2.2. Coherence

The coherence spectra,COH_{xy}, for given signals S_1 and S_2, is given as

$$COH_{S_1S_2}(f) = \frac{|C_{S_1S_2}(f)|^2}{(C_{S_1S_1}(f) \times P_{S_2S_2}(f))} \tag{2}$$

where P denotes power or cross-power. $|C_{S_1S_2}(f)|$ is the cross-spectrum between signals S_1 and S_2, while $C_{S_1S_1}(f)$and $C_{S_2S_2}(f)$are the auto-spectrum of the signals S_1 and S_2 respectively. Measure of coherence depends on both amplitude and phase of the signal with a value varying between 0 and 1 [47]. Higher coherence corresponds to two different sites of the scalp working more diligently together at a particular frequency. The EEG coherence is computed using the Welch's periodogram method with 1024 point Fast Fourier Transform (FFT) and Hanning window of epoch length.

3.2.3. Phase Synchronization Index

The phase synchronization for the given signals S_1 and S_2, is defined as

$$\varphi_{S_1,S_1}(t) = |S_1\phi_1(t) - S_2\phi_2(t)| < z \tag{3}$$

where $\varphi_1(t)$and$\varphi_2(t)$define the instantaneous phases of two given signals at time t, S_1 and S_2 are integers, and "z" is a constant. For a given signal, the phase is calculated using the Hilbert transform,

$$y(t) = \frac{1}{\pi}P\int_{-\infty}^{\infty}\frac{x(\tau)}{t-\tau}d\tau \tag{4}$$

where the original signal $x(\tau)$is transformed into its Hilbert transform $y(t)$and P denotes the Cauchy principal value. The instantaneous phase can then be calculated as:

$$\phi(t) = \arctan\left(\frac{y(t)}{x(t)}\right) \tag{5}$$

From the phases of given signals S_1 and S_2, the phase differences $\left(\text{i.e., } \phi = \phi_1 - \phi_2\right)$can be obtained. The phase synchronization index (PSI) for two given signals with epoch length$N$is defined as,

$$PSI = |\frac{1}{N}\sum_{t=1}^{L}e^{i\phi(t)}| \tag{6}$$

The measure of PSI depends on phase change and its value varies between 0 (no phase synchronization at all) and 1 (perfect phase synchronization) [48].

3.2.4. Proposed higher order spectra (HOS) based brain functional connectivity index

The Higher Order Spectra (HOS) is the spectral representation of higher order statistics of a given signal. In this research, the 3rdorder cumulant spectrum called the bispectrum is used and denoted by $Bi(f_1, f_2)$[31] which are the two-dimensional third order cumulant Fourier Transform (FT) defined as follows:

$$Bi(f_1, f_2) = \sum_{m=-\infty}^{\infty}\sum_{n=-\infty}^{\infty} c_3^X(p, q)\exp\left[-jpf_1 + qf_2\right] \tag{7}$$

where $C_3^X(m, n)$is the FT of the third order cummulant which is defined as follows:

$$C_3^X(p, q) = E\left\{X(p)X(q)X(p+q)\right\} \tag{8}$$

The bispectrum is a function of two independent frequency variables. Because of its symmetry properties [41] for a real-valued and discrete-time signal, it needs to be computed only over a triangular region in the bifrequency space as shown in [41]. The bispectrum is complex-valued and contains phase information. The phase of the integrated bispectrum along a straight line of given slope, m, in the bi-frequency space is the bispectral invariant feature, $\phi(m)$ defined by [49]

$$I(m) = \int_{f_1=0^+}^{\frac{1}{1+a}} Bi(f_1, mf_1)df_1 = I_{Re}(m) + jI_{Im}(n) \tag{9}$$

$$\phi(m) = \arctan\left(\frac{I_{Im}(m)}{I_{Re}(m)}\right) \tag{10}$$

Then, bispectrum-based PSI (bPSI) is computed as,

$$bPSI = |\phi_{m_1} - \phi_{m_2}| \tag{11}$$

where $\phi_{m_1}$and ϕ_{m_2}denote the phases of the integrated bispectrum of two given signals S_1 and S_2. The bispectrum is computed from segment of 6 s epoch (containing 768 samples) with Hanning window of 50% overlap sampled at 128 Hz.

3.3. Statistical data analysis

SPSS 20.0 software is used for performing the statistical analysis. In this study, different connectivity indices are assessed for each frequency band among all pairs of 14 electrodes using repeated measures ANOVAs with conditions as the within-subjects factor, with six levels: happiness, sadness, fear, anger, surprise and disgust and the electrode pair (with 91 pairs) as the between-subjects factor [36]. Then post-hoc Tukey test is used to study the BFC patterns under the specific emotional states of PD patients and HC. These analyses are performed separately for PD patients and HC participants.

3.4. Classification of emotions based on BFC indices using EEG

A total of 720 × 91 EEG data for each emotion in each band is obtained from 20 subjects belonging to each group who underwent six trials and six segments per channel (i.e., 20 × 6 × 6 = 720). The four functional connectivity indices are extracted from these samples and selected as feature vectors for pattern classification. In order to limit the vast space of input features, a feature selection was performed based on the sequential forward feature selection (SFFS) method [50]. Finally, a support vector machine (SVM) classifier [51–53] is used to evaluate the functional connectivity feature vectors. First, SVM maps features vectors into a high dimensional feature space using a certain kernel function [54]. Using quadratic optimization, an optimal hyper plane is found and the margin of separation between the classes is maximized. In this research Radial Basis Function (RBF) [55–58] kernel function is used. Suitable values for RBF kernel such as cost parameter (C) and kernel parameter (γ) are found through numerical experimentation. In this work, LibSVM toolbox [59] is used to perform the classification of emotional states. The 10-fold cross-validation technique is used to evaluate the performance and the reliability of the SVM classifier.

The emotional state classification results using feature vectors derived at the single-electrode EEG are also compared to the one extracted from BFC with pairwise combination of electrodes. Two methods are used to extract energy features at single-electrode EEG signals: FFT and Wavelet Packet Transform (WPT) [60,61]. In the FFT method, each EEG epoch is first processed with Hanning window and then used to compute the FFT (with 1024 points). Next, the logarithm of energy from FFT is calculated for each EEG epoch of PD patients and HC participants to be used for feature classification. In the WPT method, each EEG epoch is decomposed into sub-bands using the Daubechies 4th order wavelet ("db4") to derive energy feature for emotion classification [62,63]. Prior to classification, fea-

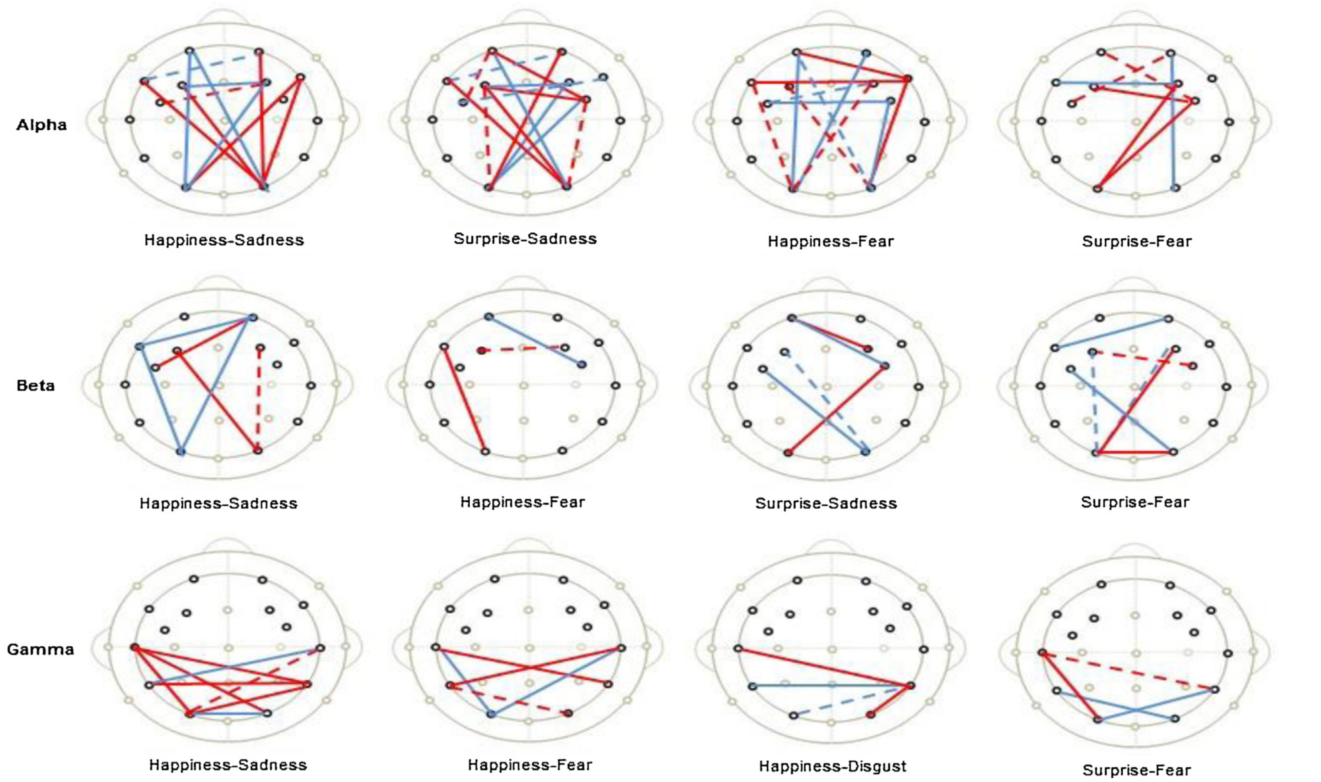

Fig. 1. Brain maps of correlation. Significant increases (solid lines) and decreases (dashed lines) of correlation in the alpha (panel 1), beta (panel 2), and gamma frequency bands (panel 3), in response to emotional stimuli. Note: Redlines denote healthy controls; blue lines denote PD patients. (For interpretation of the references to colour in this figure legend, the reader is referred to the web version of this article.)

ture vectors are normalized to the range of [01] using the Min-Max algorithm.

4. Results

4.1. Brain functional connectivity indices using EEG

4.1.1. Correlation

Table 2 shows the correlation index of emotional states. The F-test yielded significant ($p < 0.05$) results only in alpha, beta and gamma frequency distributions in HC and PD patients. Significant post-hoc Tukey test analysis between emotional states for COR is shown in Fig. 1. The red lines between electrode locations indicate higher significant value index for the condition while blue dashed lines between electrode locations indicate lower significant index values for the condition. No significant differences among emotional states are observed in delta and theta frequency bands of PD patients and HC participants. In the alpha and beta band, there are differences in connectivity patterns among frontal and occipital regions in sadness and fear emotions exhibiting larger correlation than happiness and surprise in PD patients and HC participants. Similar results are obtained in the gamma frequency band, which shows a higher correlation during sadness, fear and disgust emo-

Table 4
Significant results of F-test using phase synchronization index (PSI) between the electrode pairs ($p < 0.05$) of PD patients and healthy controls.

Frequency band	PD Patients						HC					
Theta	AF3-F3	$F = 5.56$	T7-P8	$F = 5.97$	T8-F4	$F = 2.15$	AF3-P8	$F = 3.20$	T7-P8	$F = 4.79$	O1-O2	$F = 4.97$
	F7-O2	$F = 4.93$	P7-O2	$F = 4.91$	FC6-F8	$F = 2.89$	F7-O1	$F = 3.19$	P7-P8	$F = 2.72$	O2-F8	$F = 5.49$
	F7-T8	$F = 5.78$	O1-P8	$F = 2.91$			F7-P8	$F = 3.89$	P7-FC6	$F = 3.08$	T8-F4	$F = 3.84$
							FC5-O2	$F = 2.08$	P7-T8	$F = 5.23$		
Alpha	AF3-P7	$F = 4.28$	T7–T8	$F = 1.67$	P8-F4	$F = 3.61$	AF3-O2	$F = 4.56$	T7-F4	$F = 4.53$	O1-P8	$F = 4.46$
	F7-T8	$F = 4.72$	T7-F8	$F = 4.89$	T8-F8	$F = 2.65$	F3-T8	$F = 4.66$	T7-AF4	$F = 4.67$	O1-F4	$F = 3.43$
	F7-F4	$F = 5.92$	P7-FC6	$F = 3.03$			F3-F4	$F = 2.78$	P7-O2	$F = 3.04$	P8-F4	$F = 2.29$
	FC5-P8	$F = 2.78$	O1-F8				FC5-P8	$F = 5.90$	P7-T8	$F = 3.20$	FC6-AF4	$F = 2.50$
Beta	F7-P7	$F = 3.20$	T7–T8	$F = 5.13$	P8-F8	$F = 3.653$	AF3-P8	$F = 4.76$	T7-T8	$F = 2.57$	P8-F4	$F = 3.29$
	F7-AF4	$F = 3.91$	P7-O2	$F = 2.66$	T8-F8	$F = 2.22$	F3-FC6	$F = 3.07$	P7-F8	$F = 4.56$	T8-F4	$F = 4.68$
	F3-P8	$F = 4.17$	P7-P8	$F = 3.63$	FC6-F8	$F = 4.68$	F3–F4	$F = 5.64$	O1-T8	$F = 3.94$	T8-AF4	$F = 4.36$
	FC5-T8	$F = 4.54$	O1-FC6	$F = 3.53$	F8-AF4	$F = 4.29$	F3–F8	$F = 5.09$	O2-FC6	$F = 4.34$	F4–F8	$F = 2.12$
			O1-F4	$F = 3.06$			FC5-O1	$F = 4.13$				
			O2-AF4	$F = 3.72$			FC5-O2	$F = 4.51$				
Gamma	AF3-O2	$F = 3.68$	P7-O2	$F = 3.30$	P8-T8	$F = 4.51$	F7-O1	$F = 3.59$	T7-P8	$F = 1.38$	T8-F4	$F = 5.95$
	F7-P8	$F = 4.65$	O2-T8	$F = 4.97$	T8-F4	$F = 3.02$	F7-FC6	$F = 5.38$	P7-FC6	$F = 3.29$	F4–F8	$F = 7.92$
	F3-T8	$F = 4.51$			FC6-F4	$F = 3.55$	F3-T8	$F = 5.35$	O1-T8	$F = 4.55$		
	F3–F8	$F = 4.08$			F4–F8	$F = 5.92$			O2-F8	$F = 3.40$		
	FC5-P7	$F = 6.38$							O2-AF4	$F = 5.44$		

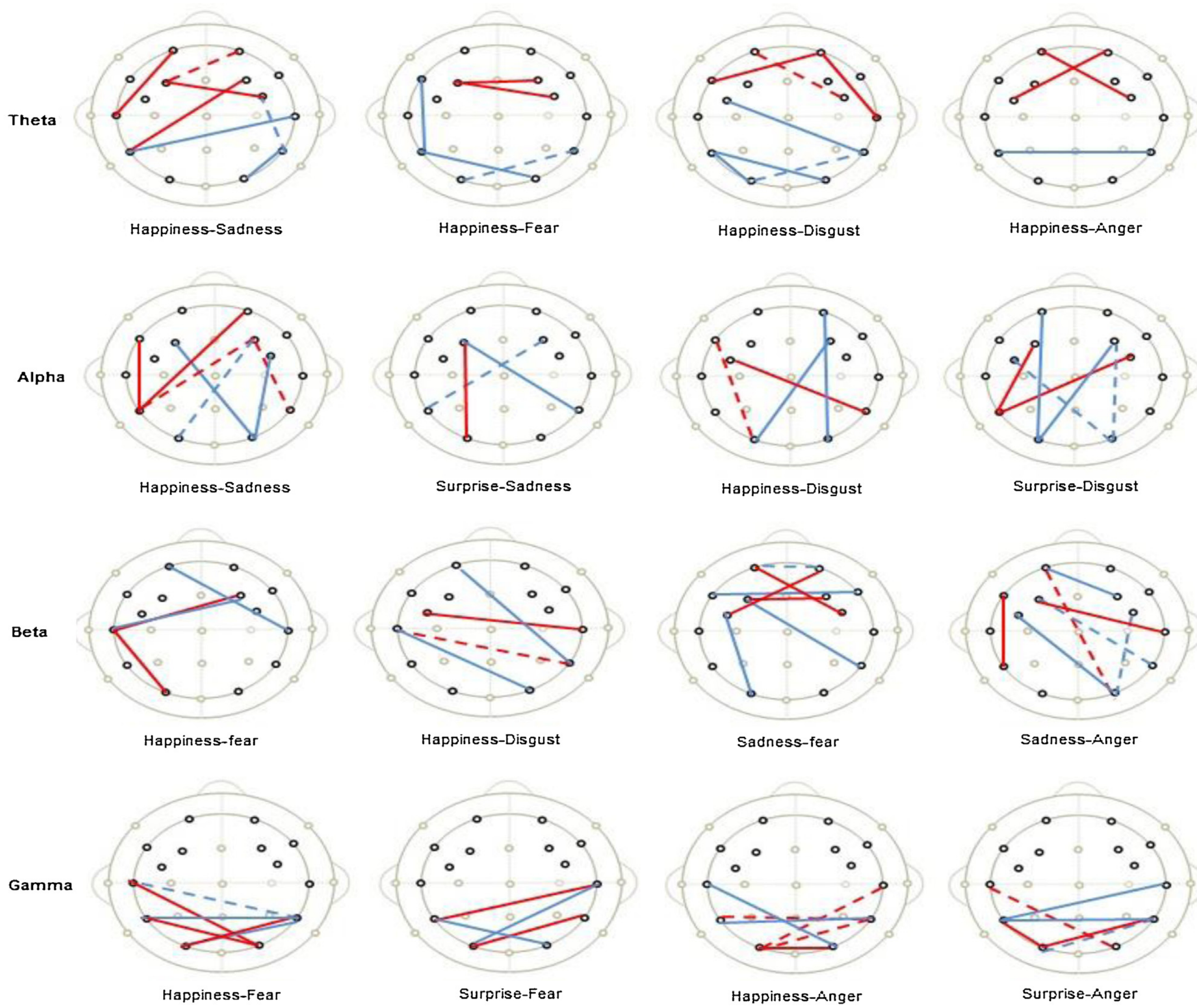

Fig. 2. Brain maps of coherence. Significant increases (solid lines) and decreases (dashed lines) of coherence in the theta (panel 1), alpha (panel 2), beta (panel 3), and gamma frequency bands (panel 4), in response to emotional stimuli. Note: redlines denote healthy controls; blue lines denote PD patients. (For interpretation of the references to colour in this figure legend, the reader is referred to the web version of this article.)

tions than happiness and surprise, mainly in the occipital, parietal, and temporal regions.

4.1.2. Coherence

Table 3 shows the coherence analysis of emotional states. The *F*-test yielded significant ($p < 0.05$) results in all the frequency bands except delta of PD patients and HC participants. Significant post-hoc Tukey test results between emotional states for COH analysis are shown in Fig. 2. No significant difference is observed in the delta band among emotional states of controls and PD patients. In the theta band, compared to happiness emotion, significant higher coherence is found in HC during sadness, fear, disgust, and anger emotion state but only at frontal sites, whereas PD patients showed higher coherence mainly at the parietal sites. In the alpha band, sadness and disgust appeared to have higher coherence than happiness and surprise emotions. However, PD patients showed interaction between the frontal and occipital regions, whereas HC participants mainly showed interaction between the frontal and temporal sites. In the beta band, significantly greater coherence is observed at the occipital and temporal regions when viewing fear and disgust emotional stimuli than happiness. We also observed significantly higher coherence during sadness emotional state than fear and anger states, mainly at the frontal sites for controls and PD patients. Similar result is obtained in the gamma frequency band, which showed a higher coherence during anger and fear emotional states than happiness and surprise, mainly at the occipital, parietal, and temporal regions.

4.1.3. Phase synchronization index

Table 4 shows the phase synchronization index of emotional states. The *F*-test yielded significant ($p < 0.05$) results in all the frequency bands except delta of PD patients and HC. Significant post-hoc Tukey test result between emotional states for PSI is shown in Fig. 3. For theta band, the surprise emotion is associated with more synchronization than sadness, fear, disgust, and anger emotion, especially showing connection in the temporal sites of PD patients, whereas HC showed greater synchronization at the frontal sites. In the alpha frequency band, the positive emotions (happiness and surprise) seemed to be more synchronized than negative emotional (sadness, disgust, and anger) responses, mainly at the occipital sites. The similar result was obtained in the beta and gamma bands, which also showed more synchronization for happiness and surprise emotional states than disgust, sadness and fear especially at the frontal and parietal regions.

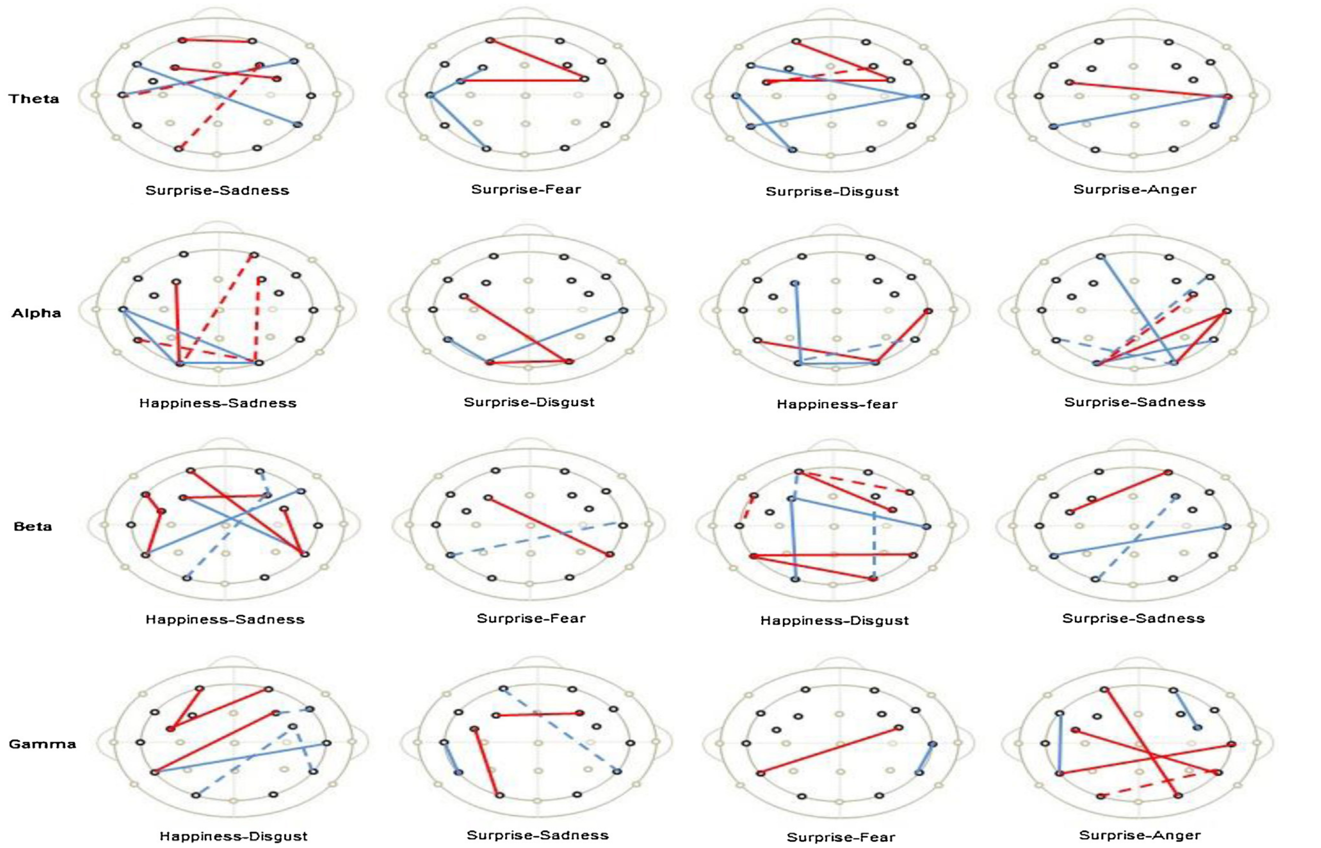

Fig. 3. Brain maps of phase synchronization index (PSI). Significant increases (solid lines) and decreases (dashed lines) of PSI in the theta (panel 1), alpha (panel 2), beta (panel 3), and gamma frequency bands (panel 4), in response to emotional stimuli. Note: redlines denote healthy controls; blue lines denote PD patients. (For interpretation of the references to colour in this figure legend, the reader is referred to the web version of this article.)

4.1.4. Bispectrum based brain functional connectivity index

Table 5 shows the bPSI of emotional states. The *F*-test yielded significant results in all the frequency bands except delta of PD patients and HC. Significant post-hoc Tukey test result between emotional states for bipsectrum based BFC is shown in Fig. 4. For theta band, the happiness and surprise emotion are associated with more synchronization than fear emotion, particularly showing connection in the parietal sites of PD patients, while HC showed greater synchronization at the frontal and parietal regions. The similar result is obtained in the alpha, beta and gamma frequency bands, which also showed more synchronization for negative emotional states than positive in HC, mainly at the frontal, temporal and parietal regions, whereas PD patients showed only at frontal regions. **.**

Classification of emotions based on BFC Indices using EEG

Tables 6–9 show the mean classification accuracy among the six emotional states of PD patients compared to HC in different EEG frequency bands with feature selection (i.e., SFFS) and without feature selection across COR, COH, PSI and bPSI connectivity indices using SVM. Several observations can be drawn from these tables.

First, the results showed BFC indices using all frequency bands (combination of five frequency bands) yielded better results than using single frequency band for both PD patients and HC participants in emotion classification. Second, the alpha, beta and gamma bands performed better than delta and theta frequency bands.

Table 5

Significant results of F-test using bispectrum based phase synchronization index (bPSI) between the electrode pairs ($p < 0.05$) of PD patients and healthy controls.

Frequency band	PD Patients						HC					
Theta	AF3-FC5	$F=5.91$	T7-P7	$F=5.29$	P8-T8	$F=8.19$	F7-FC5	$F=5.94$	P7-FC6	$F=5.29$	FC6-F4	$F=5.10$
	AF3-AF4	$F=7.29$	P7-FC6	$F=6.82$	FC6-AF4	$F=4.10$	F3-P8	$F=2.45$	O1-P8	$F=4.10$	F4-AF4	$F=4.10$
	F7-T7	$F=10.34$	O1-FC6	$F=7.29$			F3-AF4	$F=3.20$				
	F3-AF4	$F=15.39$										
Alpha	AF3-F8	$F=9.10$	T7-T8	$F=4.67$	P8-F4	$F=5.10$	AF3-O2	$F=9.20$	P7-T8	$F=1.84$	O2-F8	$F=14.48$
	F3–F4	$F=3.67$	P7-FC6	$F=6.92$	FC6-AF4	$F=4.92$	F7-P7	$F=4.83$			P8-F4	$F=10.58$
	FC5-O2	$F=4.29$	O1-T8	$F=5.20$	F4–F8	$F=6.78$	FC5-FC6	$F=7.28$			FC6-AF4	$F=17.39$
					F8-AF4	$F=4.10$					F4–F8	$F=10.24$
Beta	F7–F4	$F=6.92$	T7-O2	$F=6.70$	O2-P8	$F=7.29$	AF3-F8	$F=4.19$	T7-O1	$F=5.28$	P8-FC6	$F=5.20$
	FC5-FC6	$F=3.20$	P7-FC6	$F=7.20$	T8-F4	$F=4.29$	F7–F8	$F=3.19$	O1-FC6	$F=3.28$	F8-AF4	$F=14.29$
			P7-AF4	$F=6.20$	F4–F8	$F=5.29$						
			O1-AF4	$F=4.29$								
Gamma	F3-T7	$F=7.29$	P7-O1	$F=6.20$	O2-F4	$F=10.36$	AF3-F8	$F=7.29$	P7-F8	$F=4.10$	T8-F8	$F=6.29$
	FC5-FC6	$F=3.20$	O1-T8	$F=3.20$	P8-F4	$F=7.20$	F3-O2	$F=4.20$	O1-FC6	$F=9.93$	FC6-AF4	$F=5.20$
					FC6-F8	$F=7.92$	FC5-P8	$F=9.10$	O1-AF4	$F=3.28$	F8-AF4	$F=5.48$
					F8-AF4	$F=4.20$						

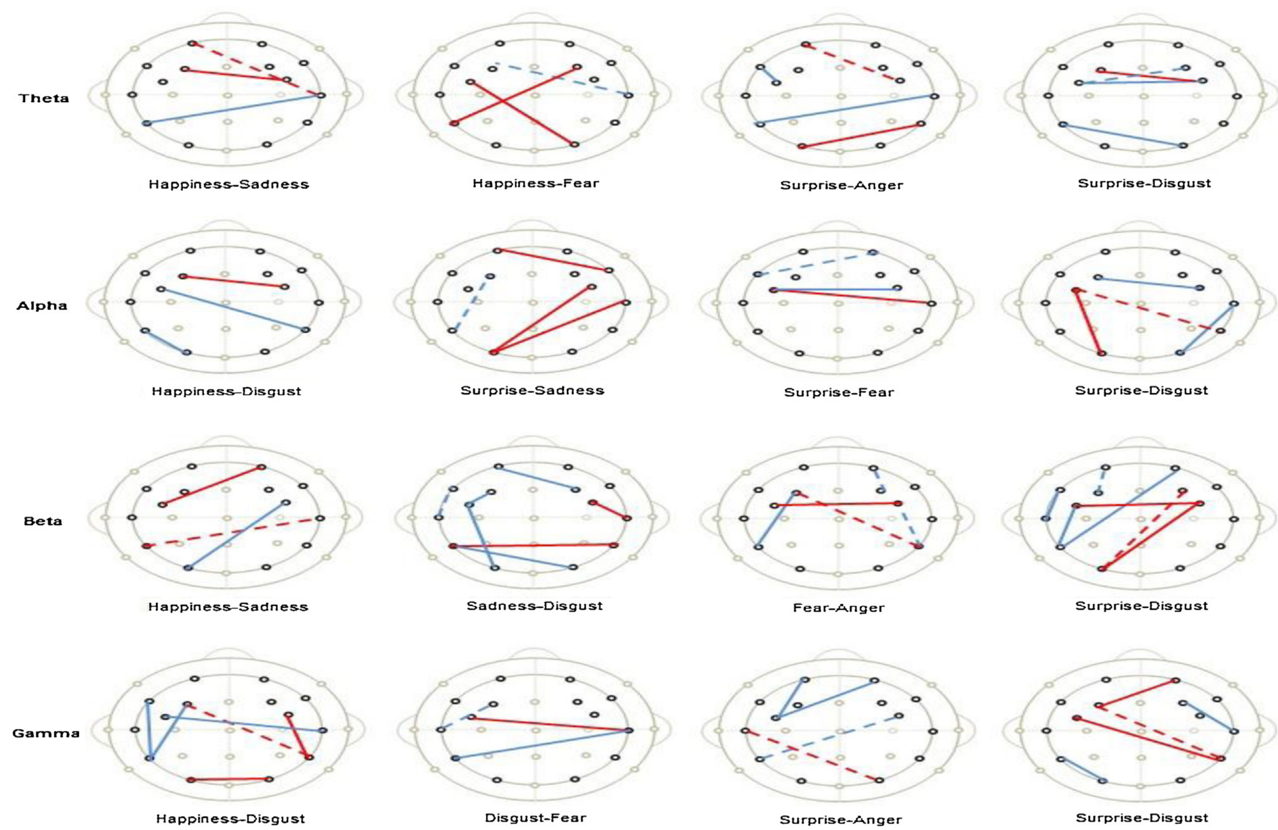

Fig. 4. Brain maps of bispectrum phase synchronization index (bPSI). Significant increases (solid lines) and decreases (dashed lines) of PSI in the theta (panel 1), alpha (panel 2), beta (panel 3), and gamma frequency bands (panel 4), in response to emotional stimuli. Note: redlines denote healthy controls; blue lines denote PD patients. (For interpretation of the references to colour in this figure legend, the reader is referred to the web version of this article.)

Table 6
Mean classification accuracy (%) in different EEG frequency bands using correlation.

Correlation	Group	Frequency band					
		Delta	Theta	Alpha	Beta	Gamma	All
Without feature selection	PD	36.76 ± 1.46	38.56 ± 2.01	43.64 ± 2.59	45.68 ± 1.08	47.88 ± 1.54	48.21 ± 1.73
	HC	46.39 ± 2.37	51.41 ± 1.42	52.42 ± 1.86	52.69 ± 2.63	54.99 ± 1.51	55.57 ± 2.03
With feature selection	PD	38.43 ± 1.06	40.47 ± 2.72	46.08 ± 1.46	46.82 ± 2.10	47.25 ± 1.49	48.94 ± 1.52
	HC	47.18 ± 1.14	52.60 ± 1.98	56.27 ± 2.16	58.50 ± 1.61	56.79 ± 1.58	60.16 ± 1.78

Note: here “All” denotes the combination of five EEG frequency band of correlation index.

Table 7
Mean classification accuracy (%) in different EEG frequency bands using coherence.

Coherence	Group	Frequency band					
		Delta	Theta	Alpha	Beta	Gamma	All
Without feature selection	PD	36.96 ± 1.49	38.99 ± 2.13	45.09 ± 2.65	47.12 ± 2.79	48.59 ± 2.01	50.97 ± 2.02
	HC	46.05 ± 2.17	46.67 ± 2.56	52.35 ± 2.44	55.59 ± 1.83	53.15 ± 1.19	55.25 ± 1.77
With feature selection	PD	40.03 ± 1.26	42.71 ± 1.45	45.76 ± 2.28	46.64 ± 2.09	49.62 ± 1.50	50.05 ± 2.22
	HC	49.08 ± 1.75	48.91 ± 2.29	54.73 ± 3.69	59.58 ± 1.43	58.59 ± 2.19	61.51 ± 1.63

Note: here “All” denotes the combination of five EEG frequency bands of coherence index.

Table 8
Mean classification accuracy (%) in different EEG frequency bands using PSI.

PSI	Group	Frequency band					
		Delta	Theta	Alpha	Beta	Gamma	All
Without feature selection	PD	43.19 ± 2.00	43.63 ± 1.40	48.25 ± 1.42	51.78 ± 2.12	51.68 ± 1.35	52.99 ± 1.81
	HC	52.36 ± 1.45	53.42 ± 2.92	60.99 ± 2.09	62.96 ± 1.86	62.67 ± 3.11	64.87 ± 2.94
With feature selection	PD	44.65 ± 1.41	45.03 ± 1.83	49.60 ± 2.68	54.27 ± 2.29	53.69 ± 1.72	50.58 ± 1.93
	HC	53.99 ± 2.82	53.56 ± 1.37	62.14 ± 2.46	64.59 ± 1.51	67.81 ± 2.26	68.93 ± 1.01

Note: here “All” denotes the combination of five EEG frequency bands of phase synchronization index.

Table 9
Mean classification accuracy (%) in different EEG frequency bands using bPSI.

bPSI	Group	Frequency band					
		Delta	Theta	Alpha	Beta	Gamma	All
Without feature selection	PD	41.22 ± 1.76	44.41 ± 1.38	48.94 ± 2.08	51.56 ± 1.63	50.58 ± 1.35	52.97 ± 2.62
	HC	53.73 ± 1.74	53.88 ± 2.21	61.17 ± 1.52	64.73 ± 1.92	65.80 ± 3.11	66.80 ± 2.03
With feature selection	PD	45.93 ± 1.33	47.50 ± 1.32	50.83 ± 2.68	53.52 ± 1.64	54.62 ± 1.53	51.66 ± 1.02
	HC	54.23 ± 1.06	54.84 ± 1. 66	63.97 ± 2.46	66.47 ± 2.60	68.71 ± 2.26	71.79 ± 1.01

Note: here "All" denotes the combination of five EEG frequency bands of bPSI.

Third, feature selection using SFFS showed better performance than those without feature selection. The topoplots (or brain maps) of Fig. 5 present the position of different electrode pairs of brain regions selected by feature selection method for classifying the emotional states of our participants. Finally, the average classification accuracy of PD patients is less compared to HC participants in all the functional connectivity indices studied.

In order to determine the best connectivity index for classification of emotional states, we compared the performance of the BFC index for combination of all frequency bands with feature selection. The result is shown in Table 10. This table indicates that, the proposed bPSI index is better than using correlation, coherence and PSI. The optimum accuracy of bPSI across most of frequency distributions using SVM is 51.66% ± 1.02% and 71.79% ± 1.01% for PD subjects and control participants, respectively.

Table 11 shows the mean classification result using feature vectors derived at single-electrode in different frequency bands. The topoplots of Fig. 6 present the positions of different single-electrode brain regions that are selected by feature selection method for classifying the emotional states of our participants. The best average classification performance is obtained with all frequency bands with feature selection, by features extracted based on FFT method: 46.16% ± 2.34% and 54.24% ± 1.49% for patients with PD and HC participants, respectively. Based on WPT analysis, we obtained 48.25% ± 1.68% and 59.04% ± 2.09% for patients with PD and HC participants, respectively.

5. Discussion

5.1. Brain functional connectivity indices using EEG

It can be observed from Tables 2–5 and Figs. 1–4 that different functional connectivity indices are observed in our all participants. In [33] a correlation analysis proposed to study the emotional changes in HC participants. The authors found increased correlation between the temporal and occipital regions during the viewing of negative emotions, thereby confirming our results.

Recently, increased coherence has been reported in HC participants during the viewing of negative emotional stimuli compared with positive stimuli [35]. Similar coherence results are reported

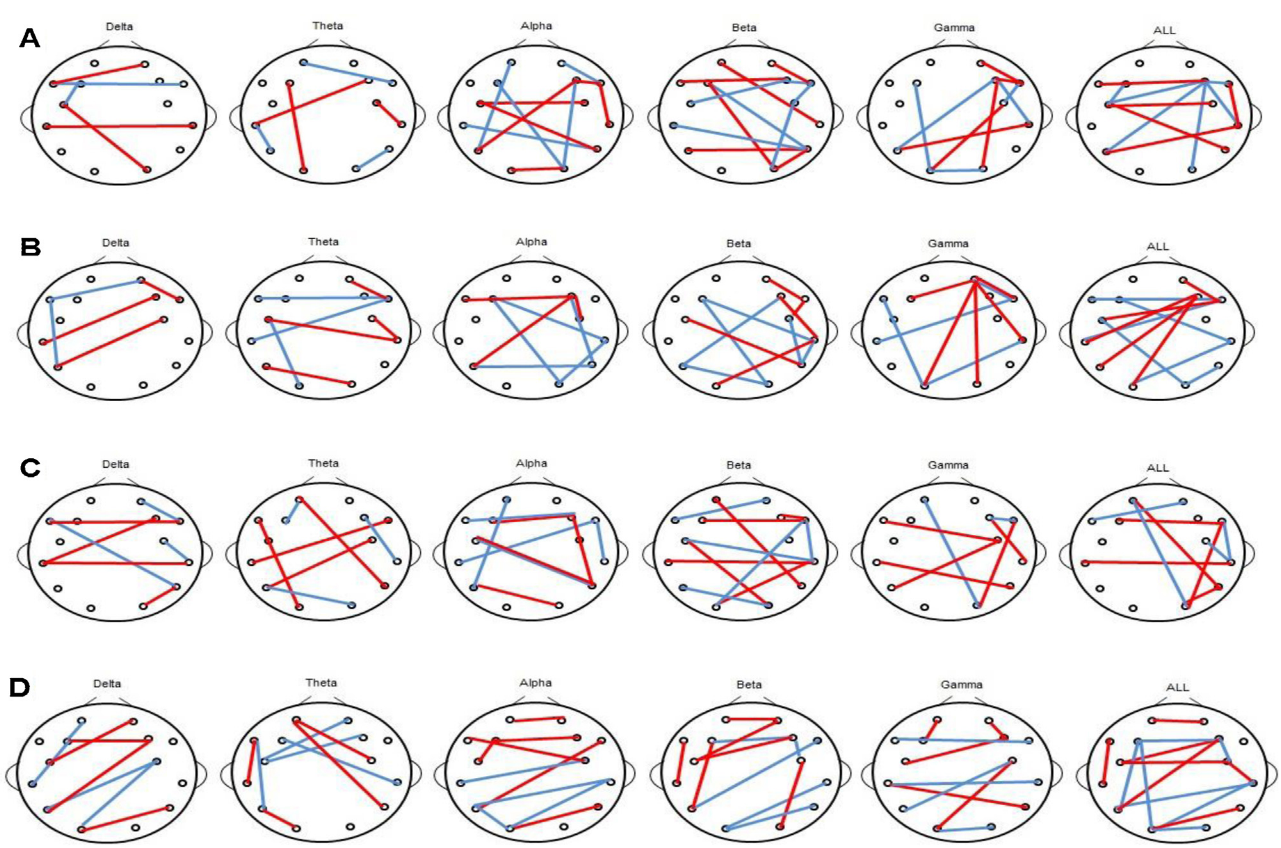

Fig. 5. Topoplots of selected features belong to EEG functional connectivity index electrode pairs and frequency band using sequential forward feature selection algorithm. (A), Correlation; (B), coherence; (C), phase synchronization index; (D), bispectrum based phase synchronization index. Note: redlines denote healthy controls; blue lines denote PD patients. (For interpretation of the references to colour in this figure legend, the reader is referred to the web version of this article.)

Table 10
Mean classification accuracy (%) comparison across all frequency bands using four brain functional connectivity indices.

	Group	Functional connectivity index			
		Correlation	Coherence	PSI	bPSI
Without feature selection	PD	48.21 ± 1.73	50.97 ± 2.02	52.99 ± 1.81	52.97 ± 2.62
	HC	55.57 ± 2.03	55.25 ±1.77	64.87 ± 2.94	66.80 ± 2.03
With feature selection	PD	50.58 ± 1.93	50.05 ± 2.22	50.58 ± 1.93	51.66 ± 1.02
	HC	68.93 ± 1.01	61.51 ± 1.63	68.93 ± 1.01	71.79 ± 1.01

Note: here "All" denotes the combination of five EEG frequency band.

Table 11
Mean classification accuracy (%) using features extracted at single-electrode level in different frequency bands.

	Group	Frequency band					
		Delta	Theta	Alpha	Beta	Gamma	All
Without feature selection							
Features based on FFT	PD	31.47 ± 2.48	34.66 ± 2.87	31.60 ± 2.64	39.11 ± 3.32	43.17 ± 2.76	41.47 ± 2.28
	HC	39.07 ± 2.12	42.53 ± 3.89	47.99 ± 2.27	44.64 ± 3.63	48.43 ± 3.54	50.94 ± 4.88
Features based on WPT	PD	33.51 ± 1.95	36.78 ± 2.29	41.81 ± 2.28	48.67 ± 2.23	48.29 ± 3.38	46.81 ± 3.65
	HC	38.83 ± 2.33	43.25 ± 2.29	50.63 ± 3.22	54.59 ± 3.76	54.26 ± 3.38	54.69 ± 2.65
With feature selection							
Features based on FFT	PD	29.90 ± 2.50	33.57 ± 2.42	37.99 ± 2.11	43.45 ± 1.70	44.86 ± 2.44	46.16 ± 2.34
	HC	40.13 ± 1.59	43.49 ± 2.11	52.90 ± 1.78	51.50 ± 2.63	49.85 ± 1.84	54.24 ± 1.49
Features based on WPT	PD	33.89 ± 2.27	39.17 ± 1.83	44.42 ± 2.15	49.34 ± 1.68	48.97 ± 2.72	48.25 ± 1.68
	HC	39.19 ± 1.67	43.73 ± 1.92	52.64 ± 1.20	55.47 ± 1.03	55.40 ± 2.42	59.04 ± 2.09

Note: here "All" denotes the combination of five EEG frequency band at single-electrode level.

in male adult participants while viewing negative versus positive video films [64]. The present findings also reveal that coherence is higher during the viewing of negative emotions than positive states in the theta, alpha, beta and gamma frequency bands for both PD patients and HC participants. Our results also confirm the earlier findings that the synchronization is higher when viewing positive emotion than negative emotion in the above mentioned EEG frequency bands of PD patients and HC participants [65]. In contrast, Costa et al. reported that sadness emotion is more synchronized than happiness emotion [36]. This discrepancy may be due to the fact that emotional stimuli used in the two studies are diverse. Kolmogorov entropy is used as a non-linear measure to investigate underlying cortical mechanisms of emotional functioning, and found that positive emotion is related with greater synchronization than negative emotion, especially at the frontal regions [66], there by confirming our findings.

Our results confirm the previous research findings that have emphasized the role of integration of brain information during emotion-related information processing. COR and COH analysis showed higher COR and COH during the viewing of negative emotions (sadness, fear, disgust, and anger) than positive (happiness and surprise), mainly at occipital and temporal regions of PD patients and HC. This shows that COR index and COH index have high degree of statistical equivalence in BFC analysis using EEG signals [47]. The PSI and proposed bPSI are smaller during negative emotional information processing than positive states. These conflicting results may be due to the contribution of dissimilarities in the computation of these four BFC indices i.e., they are sensitive to different characteristics (amplitude, phase and polarity) of the EEG signal.

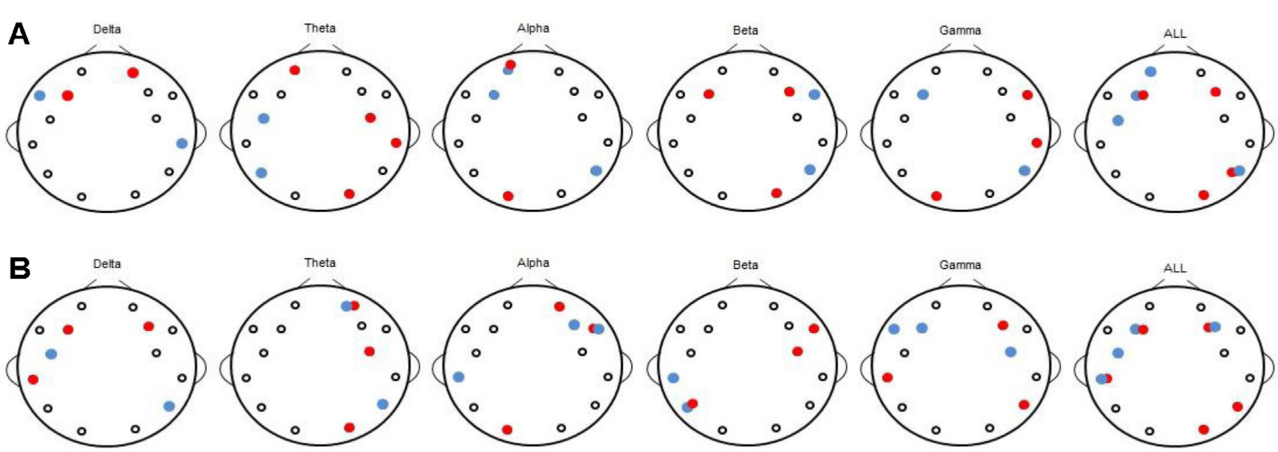

Fig. 6. Topoplots of selected features at single-electrode level across frequency band using sequential forward feature selection algorithm. (A), FFT based method; (B), WPT based method. Note: red dotes denote healthy controls; blue dots denote PD patients. (For interpretation of the references to colour in this figure legend, the reader is referred to the web version of this article.)

5.2. Classification of emotional states based on BFC indices using EEG

Tables 6–9 demonstrate that BFC indices using EEG in each frequency band reveal particular emotion patterns and can be utilized to classify different human emotional states. Similar results are reported in several emotion-related frequency band studies [23,67–69]. Furthermore, the emotion-specific connectivity index is mainly related to high frequency band (alpha, beta and gamma) than low frequency band (delta and theta) in both our participants. This partly reflects that functional connectivity indices at high frequency bands play a more important role in emotional activities than low frequency band [63,70]. In addition, high frequency band has been associated with emotional processing with in the amygdala (one of the most important brain region for emotion) [71]. Hence the distributions of high frequency band activation recorded from the scalp surface may be significant in the results for discovering links between emotional experiences and EEG recordings. Tables 6–9 also show that the classification results based on all frequency bands is better than only one frequency band. This is consistent with results of a recent study by Wang et al. [63]. Thus, we can conclude that combination of all the frequency bands of EEG signal need to be considered in emotion-related research.

Several researchers have reported that proper feature selection is needed to attain higher classification performance [63,65]. As seen in Tables 1–4, the classification using more efficient and easily interpretable features result in better performance. The performance of the pattern classification technique is improved [65]. As shown in Fig. 5, most of the electrode sites selected by SFFS are from frontal, temporal and parietal regions. These regions are associated in emotion-related activities reported in the works on neurophysiological emotional responses. Certain electrode sites from occipital region are also selected, which is described to be associated in visual processing; due to the use of multimodal emotional stimuli.

The lower emotional classification rate in PD patients using EEG signals may due to the presence of functional disconnections exist among cortical areas [72]. Our findings corroborate with past findings that, there is reduction in the brain complexity caused due to reduced connectivity of neural connections in PD patients [5,73,74].

Table 10 shows that classification performance using proposed bPSI index is better than using COR, COH and PSI. Several studies have tried directly to study the brain synchrony by computing COH measure. However, studies have noted that COH can be applied only to stationary signals since it is a measure of the linear co-variance between two given signal spectra [48,75]. In addition, COH also increases with amplitude covariance and phase covariance in the COH value is not clear [47]. Likewise, measure of COR depends on both phase and polarity of the given signal. In contrast, the PSI and bPSI are influenced only by the change of phase; however, bPSI is able to capture the nonlinear and dynamic nature of EEG signals and yielding better information about brain interactions during emotion-related information processing. Thus, classification performance is better using bPSI features. The experimental results, shown in Table 11, clearly indicate that emotional state classification performance is more accurate when using feature vectors derived from electrode pairs of BFC indices than using single electrodes. Hence, EEG-based BFC seems to be more effective in understanding the changes in brain activity during emotional processing. The advantage of the proposed emotional classification system in the clinical environment is that it is completely non-invasive and automated. This can be used to identify the emotion recognition deficits in patients with PD and to direct the patients for medical treatment, such as computerized cognitive rehabilitation. However, in order to maintain medical legal concerns, clinicians need to save all the results and EEG data. This may demand additional storage space and can degrade human decision making.

6. Limitations

Since the evaluated electrodes are relatively close to each other, it is important to rule out potential effects of volume conduction. Further research is needed to study the effect of the volume conduction artifacts using an imaginary part of coherency [76] involving a larger number of PD samples. This can enhance understanding of relationship between BFC and emotion. The PD patients in this study are affected by the motor symptoms in either side of the body (predominantly left-sided and right-sided motor symptoms). The distinction between predominantly affected sides in PD individuals should be considered in future studies. This subgroup differences within PD may provide hopeful leads for intervention and rehabilitation in emotional impairments. Moreover, all PD patients received medication which might have influenced their performance during emotion-related information processing [77]. In future studies PD patients who are not on medication may reveal the actual effect in emotion-related information processing. In addition, other multivariate functional connectivity measures called Directed Transfer Function and Partial Directed Coherence can be considered for assessing brain connectivity patterns during emotion processing [78]. Studying such methods for emotion impairments in neurological disorder may be useful in clinical investigations of PD patients. In terms of recording system, the emotive headset may have wireless data connection losses in closed areas since it's a wireless device. Also, the system needs an expert to place electrodes in specific locations on the scalp to record quality EEG signals. The electrodes can easily get corroded while using conductive gels. These limitations may reduce the performance in the emotion recognition system and needs further investigation.

7. Conclusion

This paper presents brain functional connectivity indices using EEG signals and describes the changes in brain interactions during emotion processing in PD patients compared to HC participants. The results suggest that there are different BFC patterns among six emotional states of PD patients and HC participants. A new feature, bPSI, is proposed for computing brain functional connectivity patterns using EEG. Its performance was found to be superior to three traditional methods: correlation, coherence and PSI. PD subjects show decreased dynamic cooperation between cortical areas during emotion processing. It is concluded that brain functional connectivity using EEG at different brain regions is a useful tool for understanding the emotional processing in PD patients. This also provides an important avenue in biomarker application that can track emotional impairments in PD patients.

Acknowledgements

The authors would like to thank all of the individuals who participated in this study.

References

[1] L.X. Blonder, R.E. Gur, R.C. Gura, The effects of right and left hemiparkinsonism on prosody, Brain Lang. 36 (1989) 193–207.
[2] A. Ariatti, F. Benuzzi, P. Nichelli, Recognition of emotions from visual and prosodic cues in Parkinson's disease, Neurol. Sci. 29 (2008) 219–227.
[3] C. Dara, L. Monetta, M.D. Pell, Vocal emotion processing in Parkinson's disease: reduced sensitivity to negative emotions, Brain Res. 1188 (2008) 100–111.
[4] A. Suzuki, T. Hoshino, K. Shigemasu, M. Kawamura, Disgust-specific impairment of facial expression recognition in Parkinson's disease, Brain 129 (2006) 707–717.

[5] A.D. Lawrence, I.K. Goerendt, D.J. Brooks, Impaired recognition of facial expression of anger in Parkinson's disease patients acutely withdrawn from dopamine replacement therapy, Neuropsychologia 45 (2007) 65–74.
[6] D. Bowers, K. Miller, A. Mikos, L. Kirsch-Darrow, U. Springer, H. Fernandez, et al., Startling facts about emotion in Parkinson's disease: blunted reactivity to aversive stimuli, Brain 129 (2006) 3356–3365.
[7] K.M. Miller, M.S. Okun, M. Marsiske, E.B. Fennell, D. Bowers, Startle reflex hyporeactivity in Parkinson's disease: an emotion-specific or arousal-modulated deficit? Neuropsychologia 47 (2009) 1917–1927.
[8] M.J. Wieser, A. Muhlberger, G. Alpers, M. Macht, H. Ellgring, P. Pauli, Emotion processing in parkinson's disease: dissociation between early neuronal processing and explicit ratings, Clin. Neurophysiol. 117 (2006) 94–102.
[9] R. Adolphs, R. Schul, D. Tranel, Intact recognition of facial emotion in Parkinson's disease, Neuropsychology 12 (1998) 253–258.
[10] M.D. Pell, C.L. Leonard, Facial expression decoding in early Parkinson's disease, Cogn. Brain Res. 23 (2005) 327–340.
[11] U.S. Clark, S. Neargarder, A. Cronin-Golomb, Specific impairments in the recognition of emotional facial expressions in Parkinson's disease, Neuropsychologia 46 (2008) 2300–2309.
[12] Y. Kan, M. Kawamura, Y. Hasegawa, S. Mochizuki, K. Nakamura, Recognition of emotion from facial, prosodic and written verbal stimuli in Parkinson's disease, Cortex 38 (2002) 623–630.
[13] S. Jerritta, M. Murugappan, K. Wan, S. Yaacob, Electrocardiogram-based emotion recognition system using empirical mode decomposition and discrete Fourier transform, Expert Syst. 31 (2) (2013) 110–120.
[14] K. Anderson, P.W. McOwan, A real-time automated system for the recognition of human facial expressions, IEEE Trans. Syst. Man Cybern. B Cybern. 36 (2006) 96–105.
[15] L. Kessous, G. Castellano, G. Caridakis, Multimodal emotion recognition in speech-based interaction using facial expression, body gesture and acoustic analysis, J. Multimodal User Interfaces 3 (2010) 33–48.
[16] G. Valenza, A. Lanata, E.P. Scilingo, The role of nonlinear dynamics in affective valence and arousal recognition, IEEE Trans. Affect. Comput. 3 (2012) 237–249.
[17] A. Correas, S.R. Holguín, P. Cuesta, E. Lopez-Caneda, L.M. García-Moreno, F. Cadaveira, et al., Exploratory analysis of power spectra and functional connectivity during resting state in young binge drinkers: a MEG study, Int. J. Neural Syst. 25 (2015) 1550008 (13 pages).
[18] P.C. Petrantonakis, L.J. Hadjileontiadis, Emotion recognition from brain signals using hybrid adaptive filtering and higher order crossings analysis, IEEE Trans. Affect. Comput. 1 (2010) 81–97.
[19] A. Kappas, Smile when you read this, whether you like it or not: conceptual challenges to affect detection, IEEE Trans. Affect. Comput. 1 (2010) 1672–1687.
[20] S.N. Daimi, G. Saha, Classification of emotions induced by music videos and correlation with participants' ratings, Expert Syst. Appl. 41 (2014) 6057–6065.
[21] R.J. Davidson, What does the prefrontal cortex do in affect: perspectives on frontal EEG asymmetry research, Biol. Psychol. 67 (2004) 219–233.
[22] T. Baumgartner, M. Esslen, L. Jancke, From emotion perception to emotion experience: emotions evoked by pictures and classical music, Int. J. Psychophysiol. 60 (2006) 34–43.
[23] D. Sammler, M. Grigutsch, T. Fritz, S. Koelsch, Music and emotion: electrophysiological correlates of the processing of pleasant and unpleasant music, Psychophysiology 44 (2007) 293–304.
[24] I.B. Mauss, M.D. Robinson, Measures of emotion: a review, Cogn. Emot. 23 (2009) 209–237.
[25] S. Ferdowsi, S. Sanei, V. Abolghasemi, A predictive modelling to analyse data in EEG-fMRI experiments, Int. J. Neural Syst. 25 (2015) 1440008 (15 pages).
[26] P. Piaggi, D. Menicucci, C. Gentili, G. Handjaras, A. Gemignani, A. Landi, Singular Spectrum analysis and adaptive filtering enhance the functional connectivity analysis of resting state FMRI data, Int. J. Neural Syst. 24 (2014) 1450010, 14 pages.
[27] R. Chakraborty, C.T. Lin, N.R. Pal, Sensor (group feature) selection with controlled redundancy in a connectionist framework, Int. J. Neural Syst. 24 (2014) 1450021, 21 pages.
[28] M. Ahmadlou, A. Adeli, R. Bajo, H. Adeli, Complexity of functional connectivity networks in mild cognitive impairment patients during a working memory task, Clin. Neurophysiol. 125 (2014) 694–702.
[29] Z. Sankari, H. Adeli, Probabilistic neural networks for diagnosis of Alzheimer's disease using conventional and wavelet coherence, J. Neurosci. Methods 197 (2011) 165–170.
[30] Z. Sankari, H. Adeli, A. Adeli, Wavelet coherence model for diagnosis of Alzheimer disease, Clin. EEG Neurosci. 43 (2012) 268–278.
[31] D. Serletis, P.L. Carlen, T.A. Valiante, B.L. Bardakjian, Phase synchronization of neuronal noise in mouse hippocampal epileptiform dynamics, Int. J. Neural Syst. 23 (2013) 1250033.
[32] D. Rangaprakash, X. Hu, G. Deshpande, Phase synchronization in brain networks derived from correlation between probabilities of recurrences in functional MRI data, Int. J. Neural Syst. 23 (2013) 1350003.
[33] J.H. Shin, D.H. Park, Analysis for characteristics of electroencephalogram (EEG) and influence of environmental factors according to emotional changes, in: G. Lee, D. Howard, D. Slezak (Eds.), Convergence and Hybrid Information Technology, Springer, Berlin, Heidelberg, 2011, pp. 488–500.
[34] H. Hinrichs, W. Machleidt, Basic emotions reflected in EEG-coherences, Int. J. Psychophysiol. 13 (1992) 225–232.
[35] V. Miskovic, L.A. Schmidt, Cross-regional cortical synchronization during affective image viewing, Brain Res. 1362 (2010) 102–111.
[36] T. Costa, E. Rognoni, D. Galati, EEG phase synchronization during emotional response to positive and negative film stimuli, Neurosci. Lett. 406 (2006) 159–164.
[37] S. Jerritta, M. Murugappan, K. Wan, S. Yaacob, Classification of emotional states from electrocardiogram signals: a non-linear approach based on hurst, Biomed. Eng. Online 12 (2013) 44–62.
[38] Y. Wang, W. Zhou, Q. Yuan, X. Li, Comparison of fractal features of ictal and interictal EEGs, Int. J. Neural Syst. 23 (2013) 1350028, 11 pages.
[39] Y. Zhang, W. Zhou, Multifractal analysis and relevance vector machine-based automatic seizure detection in intracranial, Int. J. Neural Syst. 2105 (25) (2015) 1550020, 14 pages.
[40] F. Su, J. Wang, B. Deng, X.L. Wei, Y.Y. Chen, H.Y. Li, Adaptive control of Parkinson's state based on a nonlinear computational model with unknown parameters, Int. J. Neural Syst. 25 (2015) 1450030, 13 pages.
[41] K.C. Chua, V. Chandran, U.R. Acharya, C.M. Lim, Application of higher order statistics/spectra in biomedical signals—a review, J. Med. Eng. Phys. 32 (2010) 679–689.
[42] C. Schroder, Z.T. Nikolova, R. Dengler, Changes of emotional prosody in Parkinsosn's disease, J. Neurol. Sci. 289 (2010) 32–35.
[43] R. Yuvaraj, M. Murugappan, M.I. Norlinah, K. Sundaraj, M.I. Omar, M. Khairiyah, et al., Optimal set of EEG features for emotional state classification and trajectory visualization in Parkinsosn's disease, Int. J. Psychophysiol. 94 (2014) 482–495.
[44] R. Yuvaraj, M. Murugappan, N.M. Ibrahim, K. Sundaraj, M.I. Omar, K. Mohamad, et al., Detection of emotions in Parkinson's disease using higher order spectral features from brain's electrical activity, Biomed. Signal Process. Control 14 (2014) 108–116.
[45] I.H. Gotlib, C. Raganathan, J.P. Rosenfeld, Frontal EEG alpha asymmetry, depression, and cognitive functioning, Cogn. Emot. 12 (1998) 449–478.
[46] H. Adeli, G. Dastidar, Automated EEG-based Diagnosis of Neurological Disorders—Inventing the Future of Neurology, CRC Press, Taylor & Francis, Boca Raton, Florida, 2010.
[47] M.A. Guevara, M. Corsi-Cabrera, EEG coherence or EEG correlation? Int J. Psychophysiol. 23 (1996) 145–153.
[48] J.P. Lachaux, E. Rodriguez, J. Martinerie, F.J. Varela, Measuring phase synchrony in brain signals, Hum. Brain Mapp. 8 (1999) 194–208.
[49] V. Chandran, S.L. Elgar, Pattern recognition using invariants defined from higher order spectra-one dimensional inputs, IEEE Trans. Signal Process. 41 (1993) 205–212.
[50] P. Pudil, J. Novovicova, J. Kittler, Floating search methods in feature selection, Pattern Recog. Lett. 15 (1994) 1119–1125.
[51] E. Castillo, D. Peteiro-Barral, B.G. Berdinas, O. Fontenla-Romero, Distributed one-class support vector machine, Int J. Neural Syst. 25 (2015) 1–17.
[52] J.S. Chou, A.D. Pham, Smart artificial firefly colony-based support vector regression for enhanced forecasting in civil engineering, Comp. Aided Civil Infrastruct. Eng. 30 (2015) 715–732.
[53] D. Li, L. Xu, E. Goodman, Y. Xu, Y. Wu, Integrating a statistical background-foreground extraction algorithm and SVM classifier for pedestrian detection and tracking, Integr. Comp. Aided Eng. 20 (2013) 201–216.
[54] U.R. Acharya, Automatic detection of epileptic EEG signals using higher order cummulant features, Int. J. Neural Syst. 21 (2011) 403–414.
[55] A. Alexandridis, R.B.F. Evolving, neural networks for adaptive soft-sensor design, Int. J. Neural Syst. 23 (2013) 1350029.
[56] H. Adeli, A. Karim, Fuzzy-wavelet RBFNN model for freeway incident detection, J. Transp. Eng. 126 (2000) 464–471.
[57] A. Karim, H. Adeli, Comparison of the fuzzy-wavelet RBFNN freeway incident detection model with the California algorithm, J. Transp. Eng. 128 (2002) 21–30.
[58] L.R. Zhou, J.P. Ou, G.R. Yan, Response surface method based on radial basis function for modelling large-scale structures in model updating, Comp. Aided Civil Infrastruct. Eng. 28 (2013) 210–226.
[59] C. Chang, C. Lin, A Library for support vector machines, 2001. Available at http://wwwcsientuedutw/∼cjlin/libsvm/.
[60] M. Murugappan, R. Nagarajan, S. Yaacob, Combining spatial filtering and wavelet transform for classifying human emotions using EEG signals, J. Med. Biol. Eng. 31 (2010) 45–51.
[61] G. Perez, A. Conci, A.B. Moreno, J.A.H. Tamames, Rician noise attenuation in the wavelet packet transformed domain for brain MRI, Integr. Comp. Aided Eng. 21 (2014) 163–175.
[62] W.Y. Hsu, Single-trial motor imagery classification using asymmetry ratio, phase relation, wavelet-based fractal, and their selected combination, Int. J. Neural Syst. 23 (2013) 1350007.
[63] X.W. Wang, D. Nie, B.L. Lu, Emotional state classification from EEG data uisng machine learning approach, Neurocomput 129 (2013) 94–106.
[64] D. Schellberg, C. Besthorn, T. Klos, T. Gasser, EEG power and coherence while male adults watch emotional video films, Int. J. Psychophysiol. 9 (1990) 279–291.
[65] Y.Y. Lee, S. Hsieh, Classifying different emotional states by means of EEG based functional connectivity patterns, PLoS One 9 (2014) 1–13.
[66] L.I. Aftanasa, N.V. Lotovaa, V.I. Koshkarova, V.L. Pokrovskajaa, S.A. Popova, V.P. Makhneva, Non-linear analysis of emotion EEG: calculation of Kolmogorov entropy and the principal Lyapunov exponent, Neurosci. Lett. 226 (1997) 13–16.

[67] R.J. Davidson, P. Ekman, C.D. Saron, J.A. Senulis, W.V. Friesen, Approach-withdrawal and cerebral asymmetry: Emotional expression and brain physiology, J. Personal. Soc. Psychol. 58 (1990) 330–341.
[68] W.J. Ray, H.W. Cole, EEG alpha activity reflects attentional demands, and beta activity reflects emotional and cognitive processes, Science 228 (1985) 750–752.
[69] Q. Luo, T. Holroyd, M. Jones, T. Hendler, J. Blair, Neural dynamics for facial threat processing as revealed by gamma band synchronization using MEG, Neuroimage 34 (2007) 839–847.
[70] D.J. Oathes, W.J. Ray, Worry, generalized anxiety disorder, and emotion: evidence from the EEG gamma band, Biol. Psychol. 79 (2008) 165–170.
[71] H. Oya, H. Kawasaki, M.A. Howard, R. Adolphs, Electrophysiological responses in the human amygdala discriminate emotion categories of complex visual stimuli, J. NeuroSci. 22 (2002) 9502–9512.
[72] A. Cronin-Golomb, Parkinson's disease as a disconnection syndrome, Neuropsychol. Rev. 20 (2010) 191–208.
[73] R. Adolphs, H. Damasio, D. Tranel, A.R. Damasio, Corticle systems for the recognition of emotion in facial expressions, J. Neurosci. 16 (1996) 7678–7687.
[74] H. Kober, L.F. Barrett, J. Joseph, E. Bliss-Moreau, K. Lindquist, T.D. Wagera, Functional grouping and cortical–subcortical interactions in emotion: a meta-analysis of neuroimaging studies, Neuroimage 42 (2008) 998–1031.
[75] B. Schack, W. Krause, Dynamic power and coherence analysis of ultra short-term cognitive processes-a methodical study, Brain Topogr. 8 (1995) 127–136.
[76] G. Nolte, O. Bai, L. Wheaton, Z. Mari, S. Vorbach, M. Hallett, Identifying true brain interaction from EEG data using the imaginary part of coherency, Clin. Neurophysiol. 115 (2004) 2292–2307.
[77] A. Tessitore, A. Hariri, F. Fera, W. Smith, T. Chase, T. Hyde, et al., Dopamine modulates the response of the human amygdala: a study in Parkinson's disease, J. Neurosci. 22 (2002) 9099–9103.
[78] L. Astolfi, F. Cincotti, D. Mattia, M.G. Marciani, L.A. Baccala, Comparison of different cortical connectivity estimators for high-resolution EEG recordings, Hum. Brain Mapp. 28 (2007) 143–157.